AD_____

Award Number: W81XWH-12-1-0591

TITLE: Organizing the Cellular and Molecular Heterogeneity in High-Grade Serous Ovarian Cancer by Mass Cytometry

PRINCIPAL INVESTIGATOR: Garry P. Nolan, Ph.D.

CONTRACTING ORGANIZATION: The Leland Stanford Junior University
Stanford, CA 94305

REPORT DATE: Oct 2014

TYPE OF REPORT: Annual

PREPARED FOR: U.S. Army Medical Research and Materiel Command
Fort Detrick, Maryland 21702-5012

REPORT DOCUMENTATION PAGE

Form Approved
OMB No. 0704-0188

1. REPORT DATE	2. REPORT TYPE	3. DATES COVERED
October 2014	Annual	30 Sep 2013 – 29 Sep 2014

4. TITLE AND SUBTITLE
Organizing the Cellular and Molecular Heterogeneity in High-Grade Serous Ovarian Cancer by Mass Cytometry

5a. CONTRACT NUMBER

5b. GRANT NUMBER
W81XWH-12-1-0591

5c. PROGRAM ELEMENT NUMBER

6. AUTHOR(S)
Garry P. Nolan, Ph.D.
Wendy J. Fantl, Ph.D.

E-Mail: gnolan@stanford.edu

5d. PROJECT NUMBER

5e. TASK NUMBER

5f. WORK UNIT NUMBER

7. PERFORMING ORGANIZATION NAME(S) AND ADDRESS(ES)
The Leland Stanford Junior University
Stanford, CA 94305-2004

8. PERFORMING ORGANIZATION REPORT NUMBER

9. SPONSORING / MONITORING AGENCY NAME(S) AND ADDRESS(ES)
U.S. Army Medical Research and Materiel Command
Fort Detrick, Maryland 21702-5012

10. SPONSOR/MONITOR'S ACRONYM(S)

11. SPONSOR/MONITOR'S REPORT NUMBER(S)

12. DISTRIBUTION / AVAILABILITY STATEMENT
Approved for Public Release; Distribution Unlimited

13. SUPPLEMENTARY NOTES

14. ABSTRACT

Primary ovarian cancer (OC) represents a complex set of stem cell and cancer cell phenotypes embedded in a mixture of stromal and infiltrating immune cells. This grant develops techniques and approaches using mass cytometry that organize the heterogeneity within and between patient tumors to enlighten mechanisms and clinical opportunities in the apparent chaotic structure of the cancer. (1) A preliminary mass cytometry OC dataset by a "social clustering" strategy finds cell neighborhoods in high dimensional space reveals that 18 out of 20 samples had clusters of apparent stem-cell expressing deterministic combinations of stem cell markers. (2) Two high dimensional antibody panels were optimized and assembled to interrogate the tumor and immune cell compartments. (3) Indivumed (Hamburg Germany) is established as source for acquiring high quality HG-SOC primary specimens from single-cell dissociated tumors obtained within 3 hours of resection. (4) A QC procedure was established that surveys tumor samples (including epithelial, mesenchymal and immune cells) prior to their resection (using Abs against cleaved cCaspase 3, cleaved cPARP, vimentin, E-cadherin and CD45) to focus resection procedures on viable non necrotic tissue. (5) Eight key cell lines which bear remarkable genetic similarity to primary HG-SOC tumors have been obtained [1] as standards for primary tumors.

15. SUBJECT TERMS
Tumor initiating cells, Modularity Optimization in Networks of Cellular Phenotypes (MONOCLE), primary diagnostic samples, Indivumed, dissociation conditions, evaluation of viability and apoptosis, immunohistochemistry, validation of tumor antibodies, validation of immune cell antibodies, ovarian cancer cell lines, future plans.

16. SECURITY CLASSIFICATION OF:			17. LIMITATION OF ABSTRACT	18. NUMBER OF PAGES	19a. NAME OF RESPONSIBLE PERSON
a. REPORT	b. ABSTRACT	c. THIS PAGE			USAMRMC
U	U	U	UU	22	19b. TELEPHONE NUMBER *(include area code)*

Table of Contents

INTRODUCTION

High-grade serous ovarian cancer (HG-SOC) is the fifth most lethal cancer in women and the most lethal of gynecological malignancies [1, 2]. Most often diagnosed at more advanced stages, a great challenge in treating HG-SOC is the apparent large number of disease subclasses based on genetic analyses [1, 3, 4]. Defective DNA repair mechanisms are characteristic of the disease and are most likely responsible for the extensive genetic abnormalities, most frequent of which are focal copy number alterations and epigenetic modifications [3, 4], confounding a systematic approach to successful treatment the disease. Furthermore, given the genetic plasticity of HG-SOC each patient can manifest one disease at diagnosis and other subtypes over time. At present, platinum-based therapeutic regimens are the most commonly used in the clinical settings of first diagnosis and post-relapse. Frequently a more aggressive platinum resistant form emerges.

According to a seminal review by Vogelstein et al. the vast array of genetic events found in cancer all converge on three essential cellular processes, cell fate, cell survival and genome maintenance all regulated by twelve intracellular signaling pathways [5]. This is consistent with cancer having a "structure".

The hypothesis of our DoD proposal was to hypothesize that in spite of the vast range of genetic aberrations detected in HG-SOC, there must exist a unifying architecture that links biology to pathology across these tumors. By dissecting HG-SOC (diagnostic, recurrent and chemoresistant) into single cells for analysis of their phenotypes and signaling states, at the *deepest possible resolution currently available*, we will provide a unifying vision of *ovarian cancer "systems biology"* to bring about more informed changes to treatment modalities. To accomplish this vision with HG-SOC, we are using a single cell technology, mass cytometry, or CyTOF (**Cy**tometry by **T**ime-**O**f-**F**light), largely developed in our laboratory, for immunologic and cancer cell studies [6-9]. CyTOF uses antibodies conjugated to chelated metal ion tags, allowing for the simultaneous measurement of up to 40 parameters on a cell-by-cell basis, including surface markers and intracellular signaling proteins. CyTOF has been applied to complex tissues such as blood, bone marrow and, recently, ovarian ascites as well as single-cell suspensions derived from primary HG-SOC tumors. Over the past year, we have profiled the tumor compartment of 16 primary HG-SOC samples and profiled the immune compartment for 10 samples with two panels of each comprised of 40 validated antibodies. We have demonstrated significant interplay between these two compartments. In addition, our lab and the Neel Lab have initiated the development of functional assays that will be used to understand which cell subsets harbor phenotypes associated with malignancy, metastasis, drug resistance and immuno-suppressive or immuno-enhancive characteristics. Furthermore, the Nolan Lab and Pe'er labs have developed a number of new data analysis tools. This information is essential for permitting early diagnosis, chemoprevention, risk assessment, development of new therapies and personalized treatment regimens for this deadly disease. An overview of our data from the last year will be presented. A brief update (bullet points) for each subtask will be given. Within the body of the text, a detailed discussion will be provided for our progress over the last year, which continues to build on **Task 1** as well as report on studies initiated for **Task 2** and some exciting new findings in our tumor immune studies in **Task 3.**

KEYWORDS

Serous ovarian cancer, primary tumors, mass cytometry, single cell, antibodies, stem cell, immune compartment, clustering, correlation analyses, NK cells, macrophages

OVERALL PROJECT SUMMARY

A. Background

Single mass cytometry facilitates high-dimensional, quantitative analysis of the effects of bioactive molecules on cell populations at single-cell resolution [6-9]. Datasets are generated with antibody panels (up to 40) in which each antibody is conjugated to a polymer chelated with a stable metal isotope, usually in the Lanthanide series of the Periodic Table [6, 8-10]. The antibodies recognize surface markers to delineate cell types, such as immune, epithelial, mesenchymal, and intracellular signaling molecules demarcating multiple cell functions such as survival, DNA damage, cell cycle and apoptosis. By measuring all these parameters simultaneously, the signaling network state of an individual cell can be measured. The ultimate goal of this work, and beyond, will be to assign molecular status and function to cell subsets defined by 40 parameters at the single cell level.

B. Overview of status of tasks

Task 1

Subtask 1a. Establish conditions for dissociation of solid tumors into single cells that maintain cells' ability for functional signaling. **Done with protocols transferred to Indivumed Inc, Hamburg Germany and now routine.**

Subtask 1b. Select a panel of extracellular modulators with which to measure signaling responses in both tumor cells and peripheral blood cells. **A preliminary list of modulators has been made including but not limited to, TBFβ, BMP2, EGF, TGFα, heregulin, amphiregulinn, LPA, IL6, LPS, IL6, IGNa, and IFNg has been made and protocols for exposing single cell dissociation of primary tumors are in the process of being transferred to Indivumed. Work in progress is prioritizing this list.**

Subtask 1c. Select two panels of ~40 antibodies each. Done. **We constructed two antibody panels in which the second was a variant of the first based on a mass cytometry experiment with six primary samples. *The data from two independent experiments with each panel will be described in the body of the text.***

Subtask 1d. We have submitted the necessary HRPO (IRB) and the ACURO and are awaiting approval. **Done**

Subtask 1e. Acquire 10 primary diagnostic (no treatment) ovarian tumor or ascites samples with matched blood samples. **Done. We have performed two mass cytometry experiments: i) six primary naïve tumors and ten HG-SOC ovarian cell lines described to be genetically most similar to primary HG-SOC [11].**

Subtask 1f. Develop and apply new informatics tools and algorithms to the data generated from subtask 1d (Nolan lab and Pe'er lab at Columbia) (these efforts will be ongoing throughout most of the duration of this award) **New tools developed: from the Nolan Lab: Citrus [12], X-shift (unpublished), Gatefinder (unpublished), Pe'er Lab: DREMI [13].**

Subtask 1g. Pending data from subtask 1e modify antibody panels. Titrate any new antibodies (3-36 months. Anticipate continuous low-level activity for this subtask throughout the award period). ***See subtask 1c.***

Subtask 1h. Acquire >er than 150 primary diagnostic (Neel lab at UHN Toronto, and Berek at Stanford) serous ovarian cancer samples (from Neel at UHN and Berek at Stanford) and process for mass cytometry with modified panels (6-40 months). Twenty five of these will be processed for xenotransplant (the Neel Lab currently has Research Ethics Board approval to conduct all of the tests described), requiring 10 mice for each subject tumor for 250 mice. **In progress.**

Subtask 1i. Using SPADE and other algorithms, segregate and aggregate cell subsets in hierarchical pattern with intracellular and cell surface marker combinations. ***Using a new***

deterministic K-nearest neighbor-clustering algorithm, we see important relationships between tumor cell subsets. This information will be presented in the body of the text.

Subtask 1j. Building of subset space in relationship to therapy/outcome (6-48 months). **We have not run enough samples and also for those we have run, not enough time has elapsed to fully evaluate patient outcome.**

Subtask 1k. Assess relative tumor-initiating properties of cell subsets from subtask 1h with established quantitative xenograft assay (Neel lab, 6-40 months). **In progress.**

Task 2

Previous work from the Nolan group showed that measuring the signaling responses of cancer cells to perturbations is more informative than assessing basal phosphorylation states. This task is focused on measuring signaling responses to extracellular perturbants such as growth factors, cytokines and drugs with relevance to ovarian cancer. In this task, the objective will be to uncover druggable pathways in serous ovarian cell subsets within and across primary samples.

Task 2 has subtasks that are dependent and independent of Task 1. For Task 2 we have set up foundational studies to measure drug responses in HG-SOC cell lines. Specifically, we have set MTT assays (colorimetric readout) to measure the effects of drugs on proliferation, and growth in soft agar assays. We are evaluating carboplatin and paclitaxel and other investigational agents such as PARP inhibitors, JQ1 (an epigenetic modifier) and others that are under evaluation based on our primary tumor work in Task 1. Due to the relative immaturity of these studies, we will focus this report on the 1c, g and i.

Task 3

Although the presence of infiltrating cytotoxic T cells correlates with good prognosis, whereas regulatory T cells correlate with poor prognosis in SOC, there is limited understanding of the factors that contribute to the generation of these opposing responses. Understanding the mechanisms by which a given tumor microenvironment is able to promote immune surveillance could eventually lead to the clinical development of biomarkers that could select patients responsive to immune therapy. We will use mass cytometry to evaluate the tumor microenvironment in the same SOC samples as above utilizing antibodies against immune cell subsets.

Subtask 3a. Assemble panel of extracellular modulators based on the known biology of the cell types that infiltrate ovarian tumors; immune cells, endothelial cells and stromal cells. **Within our tumor panel, we included antibodies against CD45 (recognizes immune cells subsets), fibroblast activating protein (FAP) (recognizes stroma) and CD31 (recognizes tumor angiogenic component) to evaluate an enriched tumor component in the primary samples. *We developed and validated a panel of 40 antibodies against the tumor immune system.* This data will be discussed within the body of this report.**

Subtask 3b. Validate reagents to monitor signaling pathways mediated by extracellular modulators in cell lines and peripheral blood. (1-24 months). **We have available a large repository of agents (growth factors, cytokines and drugs [14]) with which to characterize immune cell subsets from peripheral blood taken from HG-SOC patients. We are currently prioritizing which agents to use.**

Subtask 3c. Acquire 10 primary serous ovarian cancer samples with which to test response of tumor infiltrating cells to extracellular modulators identified in 3a. **(Ongoing).**

Subtask 3d. Culture tumor-infiltrating lymphocytes from samples in Subtask 3c and characterize them for cytokine and chemokine production. (Ohashi lab 12-24 months). **This subtask has changed and the Nolan Lab is generating enriched immune fractions from primary tumors**

and establishing in vitro assays to determine immune-suppressive versus immune-enhancive activities of the tumor immune compartment.

Subtask 3e*:* Acquire >er than 150 primary serous ovarian cancer samples (Neel lab at UHN Toronto, and Berek at Stanford) with which to test response of tumor infiltrating cells to extracellular modulators identified in 3a. (24-50 months). **In progress.**

Subtask 3f*.* Culture tumor-infiltrating lymphocytes from samples in Subtask 3c and characterize them for cytokine and chemokine production. (Ohashi lab 24-60 months). **See Subtask 3d.**

Subtask 3g*:* Using SPADE and other algorithms, segregate and aggregate tumor infiltrating cell subsets in hierarchical pattern with intracellular and cell surface marker combinations. Build computational models that correlate intracellular signaling responses in tumor infiltrating cell subsets with intracellular signaling responses of tumor cells with clinical outcomes. (12-60 months) ***In progress and update will be in body of text.***

C. Description of studies and results

C.1 As in our first year, we continue to pay close attention to obtaining samples of the highest quality, minimizing their ischemic time. With Indivumed Inc. in Hamburg we have highly stringent protocols in place that are now routine. All the primary samples that we evaluated were processed within 4 hours including transit time. *We believe these initial steps—though tedious—are critical to "trusting" the data from such precious samples as those obtained from patients with fatal diseases.* As an illustration of the quality of our data Table 1, last two columns in red, demonstrates comparable viability of samples pre-freeze (trypan blue) with the viability post-mass cytometry experimentation (cisplatin [15]). All samples were processed in duplicate and some in quadruplet (discussed below)

Sample ID	CyTOF 1	CyTOF 2	CyTOF 3	CyTOF 4	CyTOF average	Pre-freeze
OC-Z500	87.22	85.54			86.38	67
OC-Z467	83.09	79.72			81.41	66
OC-Z367	85.11	82.75			83.93	74
OC-Z377	77.96	77.11			77.54	73
OC-Z393	48.83	48.78			48.81	66
OC-Z403	53.28	54.58			53.93	64
OC-X2638	75.09	71.35	73.97	74.67	73.77	74
OC-X2648	85.06	81.96	82.54	83.28	83.21	80
OC-Z378	60.24	58.44	57.82	58.62	58.78	85
OC-X2643	76.64	78.71	82.23	82.59	80.04	79

Table 1: Comparable viability of samples pre-freeze (trypan blue at Indivumed) with viability post-mass cytometry experimentation (cisplatin at Stanford).

C.2a Experimental Design

Experiment #1.

Using the tumor antibody panel we included in our report last year, we performed an experiment with six primary HG-SOC samples and ten HG-SOC cell lines and one leukemic cell line as a negative control. We used the data to modify the tumor panel including more antibodies against surface proteins and included HE4, which has high relevance to HG-SOC a prognostic marker. This panel was used to characterize 10 primary HG-SOC samples and ten HG-SOC cell lines. For two tumors, we have in excess of 50 million cells and these tumors will be used later to isolate cell subsets for functional studies. For the purposes of clarity, we will discuss the data from the second experiment, although it should be pointed out, that results from the first experiment were reproduced in experiment #2.

In designing our experiments, we paid close attention to generating reproducible data. Therefore, multiple replicates were built in to the experimental design in order to compare sample runs within an experiment and across experiments. The latter being the same experiment performed on a different day.

To reduce sample-to-sample variability, mostly due to staining with the antibody panel and differences in machine sensitivity, cells corresponding to each sample were barcoded using 6 stable palladium isotopes with a method similar to that described previously [14]. In the barcoding scheme, each isotope is used in binary fashion, high for "1" and low for "0". Hence, the barcode itself is a binary string that is can be decoded for each cell to determine the sample from which each cell is derived. For the purpose we developed an error-correcting 3-one barcoding scheme that both facilitates ease of debarcoding, and eliminates the majority of cell-cell doublets. For the algorithm to be enabled, the maximum number of barcoded samples that can be combined is 20. This work is in press Zunder, Finck, et al. Nature Methods and as such is a valuable asset to those in the scientific community performing mass cytometry studies.

For the experimental set-up, 1 x 10^6 cells from each sample or cell line were portioned into a well of a barcode plate. There were two plates, each with a duplicate, that were processed for mass cytometry with either the tumor antibody panel or the immune antibody panel (Table 2 and 3). The entire experiment was repeated the following week.

Protein	Biology	Isotope	Protein	Biology	Isotope
FAP	Stroma	In113	Ki67	Cell cycle	Sm152
CD31	Angiogenic	In113	pRb(S807/811)	Cell cycle	Ho165
CD45	Immune	Ce140	Cyclin B1	Cell cycle	Nd148
E-Cadherin	Epithelial	Gd158	pHH3(S28)	Cell cycle	Yb176
CD73	Immune suppressive/Lineage plasticity	Pr141	pATM(S1981)	DDR	Nd146
CD61	Stem cell marker	Nd142	pH2AX(S139)	DDR	Sm147
CD90	Stem cell marker	Nd144	pERK(T202/204)	Proliferation	Eu151
CD151	Adhesion	Nd151	pAKT(S473)	Survival	Tb159
CD49f	Stem cell marker	Eu153	prpS6(S235/236)	Protein translation	Yb172
CD133	Stem cell marker	Gd155	pBcl2(S70)	Survival	Nd150
CD10	Exopeptidase	Gd156	pSTAT3(Y705)	Pleiotropic	Sm154
CD13	Exopeptidase	Er168	pSTAT5(Y694)	Pleiotropic	Dy162
Endoglin	TGFbRIII/Resistance/Self-renewal	Dy163	p65 Rel-A(S529)	Pleiotropic	Sm149
CD24	Stem cell marker	Dy164	MYC	Yamanaka factor	Dy161
CD44	Stem cell marker	Er166	SOX2	Yamanaka factor	Gd160
CA125	Ovarian specific	Nd143	Non-P-b-catenin	Self-renewal/Adhesion	Er170
Mesothelin	Ovarian specific	Yb173	SNAIL	Mesenchymal transition	Gd157
Vimentin	Intermediate filament/mesenchymal	In115	PAX8	Lineage specific oncogene	Er167
HE4	Protease inhibitor/biomarker for OC	Tm169	pCREB(S133)	Pleiotropic	Yb174
cleaved PARP	Apoptosis	Yb171	p53(total)	Cell cycle/Genome integrety	Lu175

Table 2: Antibody panel directed at tumor compartment

Thus, in total there were eight "runs" all of which were normalized to bead standards [16] and debarcoded.

Protein	Biology	Isotope	Protein	Biology	Isotope
CD235	Erythroid cells	In113	HLA-DR	DCs/B cells/monocytes	In115
CD66b	Granulocytes	Dy161	CD33	Myeloid/Monocytes	Gd158
CD45	Lymphoid/Myeloid	Ce 140	CD14	Monocytes/Macrophages/DCs	Gd160
CD19	B cells	Gd 155	CD11b	Grans/Monocytes/Macrophages/DCs	Nd144
CD3	T cells	Er170	CD11c	Monocytes/cDC	Gd157
CD4	T cells	Nd145	CD68	M1 & M2 macrophages	Eu167
CD8	T cells	Nd146	CD163	M2 Macrophages	Eu169
CD45RA	Naïve T & Teff cells	Eu153	CD206	M2 Macrophages	Nd150
CD25	T regs	Tm169	pSTAT1(Y701)	Transcriptional program	Nd143
FoxP3	T regs	Er166	pSTAT3(Y705)	Transcriptional program	Sm154
CCR7	Naïve & Tcm cells	Tb159	pSTAT5(Y694)	Transcriptional program	Dy162
LAG3/CD223	Immunosuppressive	Yb173	pERK(T202/Y204)	Proliferation	Eu151
PD-1	T cells (negative regulator)	Lu175	prpS6(S235/236)	Protein translation	Yb172
ICOS	Activated T cells, Co-stimulatory receptor	Dy164	pMAPKAPK2(T334)	Stress/inflammatory response	Nd142
CCR6	Lymphocyte migration, Th1/Th2/Th17 differentiation	Pr 141	pNFkB	Inflammation/survival/apoptosis	Sm149
CXCR3	Chemotaxis, Th1/Th2/Th17 differentiation	Dy163	pH2AX(S139)	DNA damage	Sm147
CD56	NK cells	Yb 176	pCREB(S133)	Transcriptional regulation	Yb174
CD16	NK cells/monocytes	Ho 165	cPARP	Apoptosis	Yb171
CD123	pDCs	Nd148	Ki67	Proliferation	Sm152
BDCA2	pDCs	Gd156			

Table 3: Antibody panel directed against immune compartment of tumor

C.2b Results from analyzing the tumor compartment

The data from the replicates was for the most part superimposable. In the first of our ongoing analysis, we used a new unpublished K-nearest neighbor's density-based clustering algorithm (Samusik, Nolan manuscript in preparation). Cells were clustered based on the co-expression of the markers shown by the grey bracket in Table 2. The clusters were arranged on a minimum spanning tree (MST) such that clusters most resembling each other were placed next to each other. In the analysis, cells from all the samples were clustered together and then each sample was viewed within the context of the others. Notably, one sample was a consistent outlier, Z393, and was actually a relapse sample

and, as such provides hypothesis-generating information. Several exemplary MSTs will be shown below, although we have generated MASTs for each protein expressed by the tumor.
HG-SOC is an epithelial cancer whose cells undergo dynamic and reversible transitions between multiple phenotypic states, the extremes of which are defined by the expression of epithelial and mesenchymal proteins. Two proteins that are hallmarks of these states are E-cadherin and vimentin respectively [17-20]. Figures 1 and 2 show the MSTs for E-cadherin and vimentin expression with striking exclusivity in their expression profiles. There are a few "bridge" areas of small clusters where both markers are co-expressed suggesting a transitional state between epithelial and mesenchymal. Notably, the relapse sample exhibits high vimentin expression consistent with a mesenchymal phenotype.

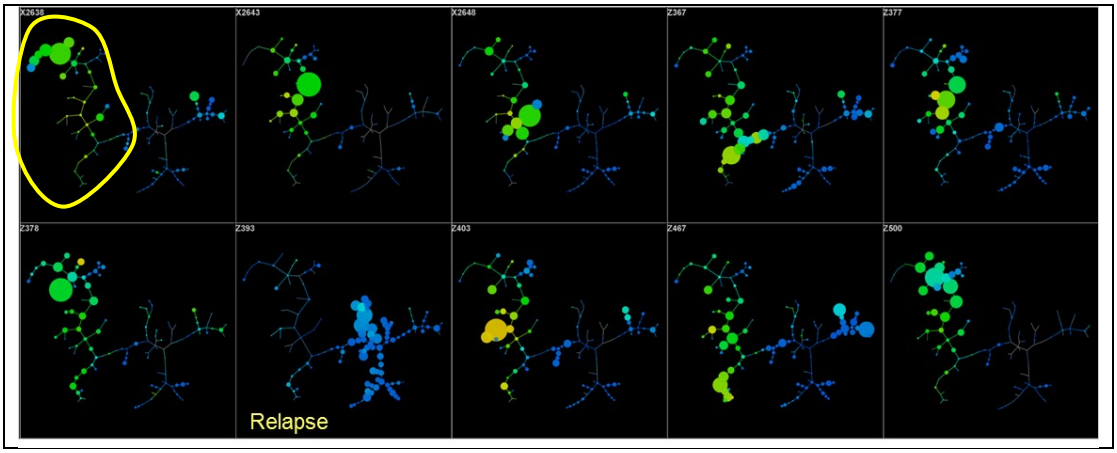

Figure 1: Minimum spanning tree shows **E-cadherin** expression confined to one part of tree and mutually exclusive with vimentin. Scale is colored from 0 (blue) to 896 (red) and represents 0 to 95th percentile of the marker intensity distribution of individual cells. Each cluster is an average of the distribution of a marker. The yellow boundary demarcates the E-cadherin compartment of the MST.

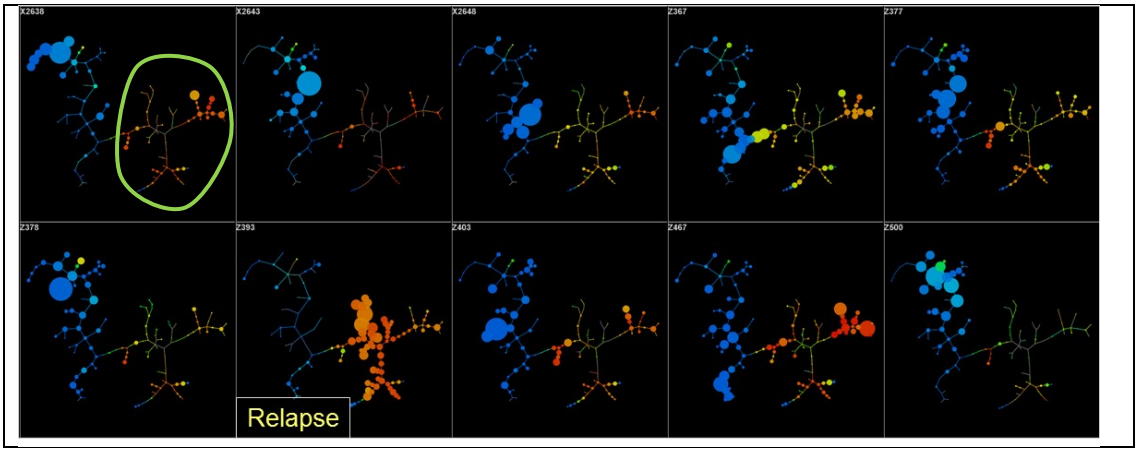

Figure 2: Minimum spanning tree shows **vimentin** expression confined to one part of tree and mutually exclusive with E-cadherin. Scale is colored from 0 (blue) to 3900 (red) and represents 0 to 95th percentile of the marker intensity distribution of individual cells. Each cluster is an average of the distribution of a marker. The green boundary demarcates the vimentin compartment of the MST.

Another striking observation from the MSTs is that there is diverse expression (distribution and level) of both these proteins across the samples, and yet all the samples fall within a regiment of hierarchies.
Included in the panel were three antibodies that recognize proteins important in the prognostication of HG-SOC, namely CA125, mesothelin and HE4 shown in Figures 3, 4 and 5. CA

125 is overexpressed in 80% of ovarian cancers. Serum CA 125 levels have been elevated in 50% to 60% of patients with stage I ovarian cancer and in 90% of patients with stage III/IV disease, related to release of CA 125 not only from cancer cells, but also from the inflamed peritoneum. In patients with elevated CA 125 levels, changes in biomarker levels have tracked tumor burden with greater than 90% accuracy. Persistent elevation of CA 125 following chemotherapy has correlated with residual ovarian cancer in >90% of cases, leading to approval of CA 125 by the US Food and Drug Administration (FDA) for detection of disease that has survived primary chemotherapy [21]. However, CA125 falls short in its ability to detect recurrent disease with enough lead-time to be useful. For this reason human epididymus protein 4 (HE4) has emerged as another serum marker and is FDA-approved to monitor recurrent disease [21]. Although serum levels of mesothelin did not offer additional advantages over CA125 and HE4 to monitoring HG-SOC [22], its restricted expression pattern to tumors, including pancreatic, compared to normal tissues have made it an attractive potential target for immuno-therapy [23-25]. Therefore, an understanding of expression patterns of these proteins at the single cell level will greatly enhance our understanding of their utility as clinical markers. Their levels in matched serum samples from the same patients is pending. The data in figures 4, 5 and 6 show that CA125 and mesothelin are co-expressed with the E-cadherin compartment whereas HE4 is more prevalent within the vimentin-expressing compartment.

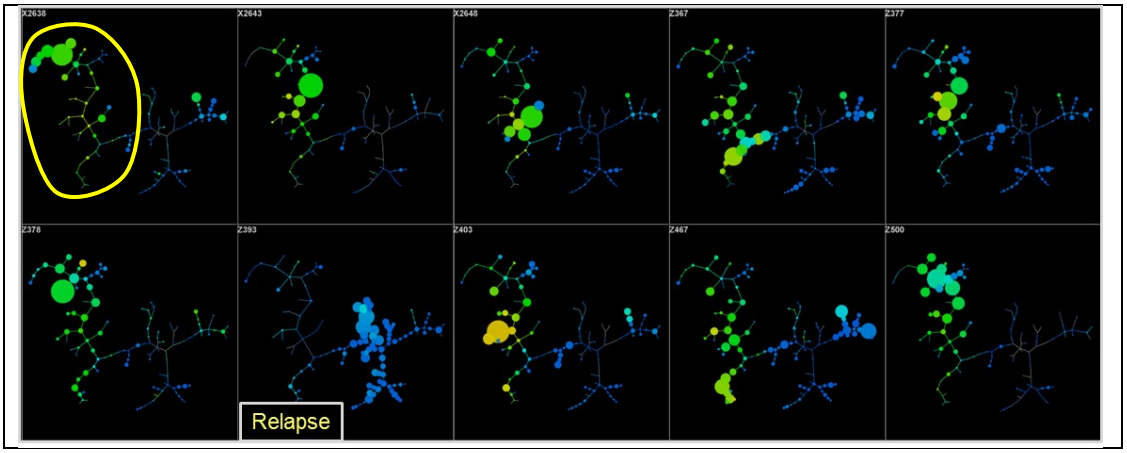

Figure 3: Minimum spanning tree shows **CA125** expression. Scale is colored from 0 (blue) to 976 (red) and represents 0 to 95th percentile of the marker intensity distribution of individual cells. The yellow boundary demarcates CA125 co-expression with the E-cadherin compartment of the tumor.

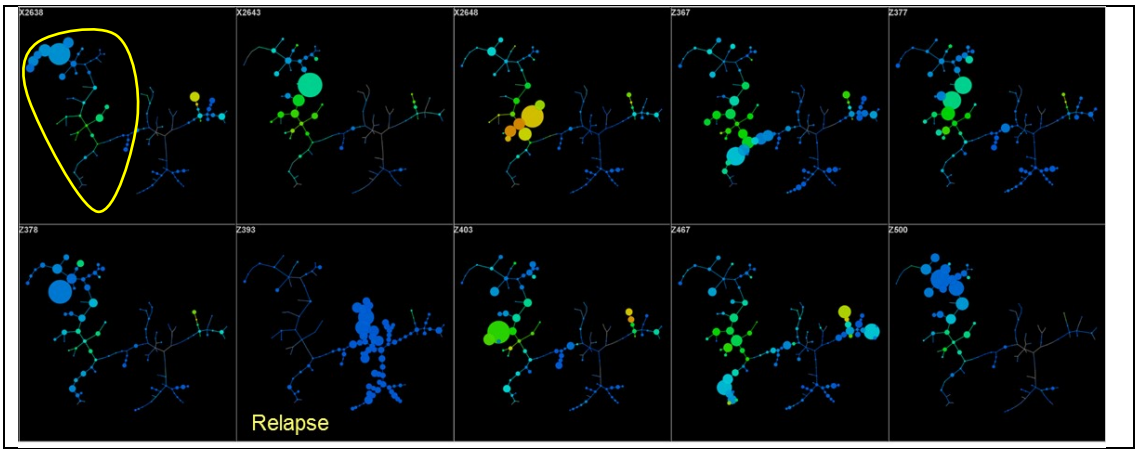

Figure 4: Minimum spanning tree shows **mesothelin** expression. Scale is colored from 0 (blue) to 2400 (red) and represents 0 to 95th percentile of the marker intensity distribution of individual cells. The yellow boundary

demarcates mesothelin co-expression with the E-cadherin compartment of the tumor. Sporadic clusters of mesothelin-expressing cells appear in vimentin part of MST.

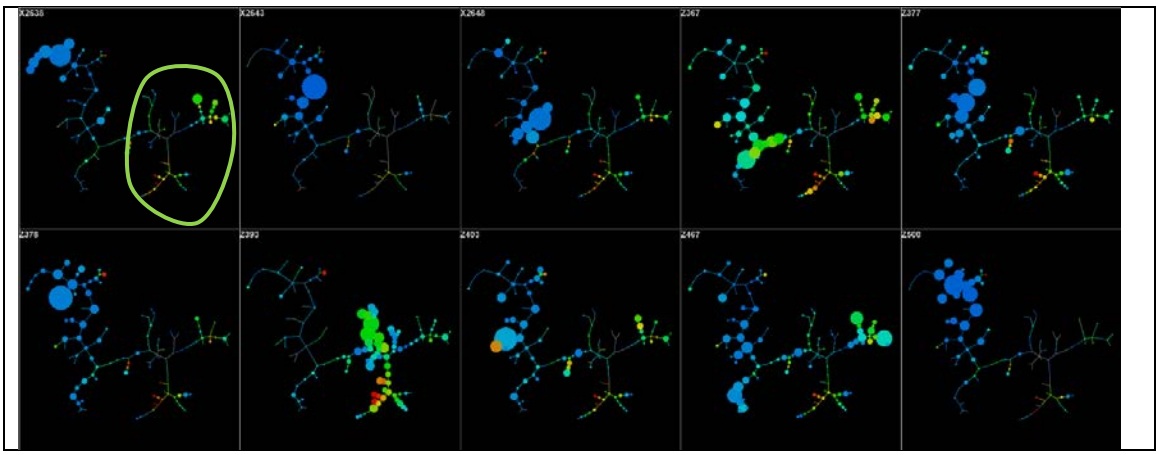

Figure 5: Minimum spanning tree shows **HE4** expression. Scale is colored from 0 (blue) to 2400 (red) and represents 0 to 95th percentile of the marker intensity distribution of individual cells. The green boundary demarcates HE4 co-expression with the vimentin compartment of the tumor.

A major goal of this project is to identify tumor-initiating cells as well as to establish a hierarchy for HG-SOC. Thus, a variety of stem cell markers were measured in each primary tumor (Table 1). Exemplary MSTs show expression patterns for the Yamanaka factors cMyc, and Sox2.

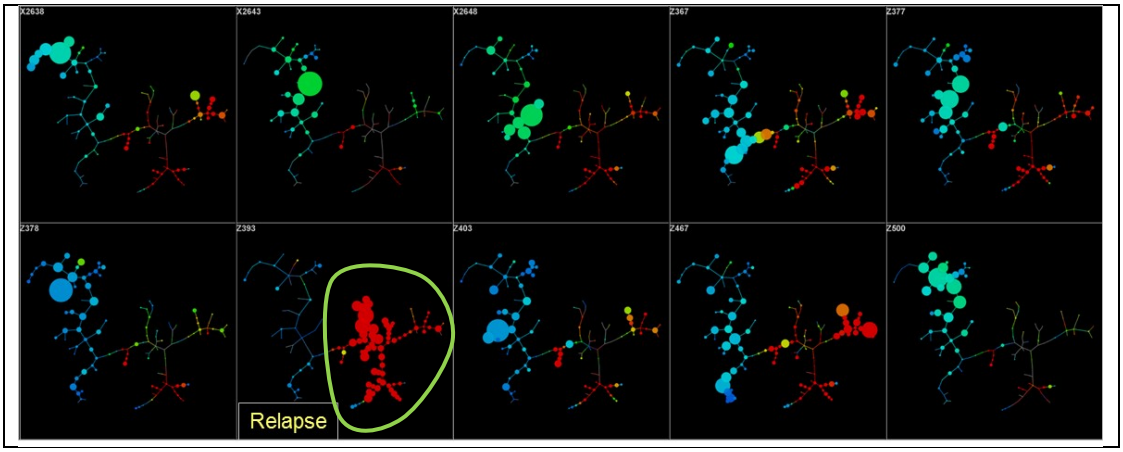

Figure 6: Minimum spanning tree shows **cMyc** expression. Scale is colored from 0 (blue) to 104 (red) and represents 0 to 95th percentile of the marker intensity distribution of individual cells. The green boundary demarcates cMyc co-expression with the vimentin compartment of the tumor. Note prominent cMyc expression in the relapse tumor.

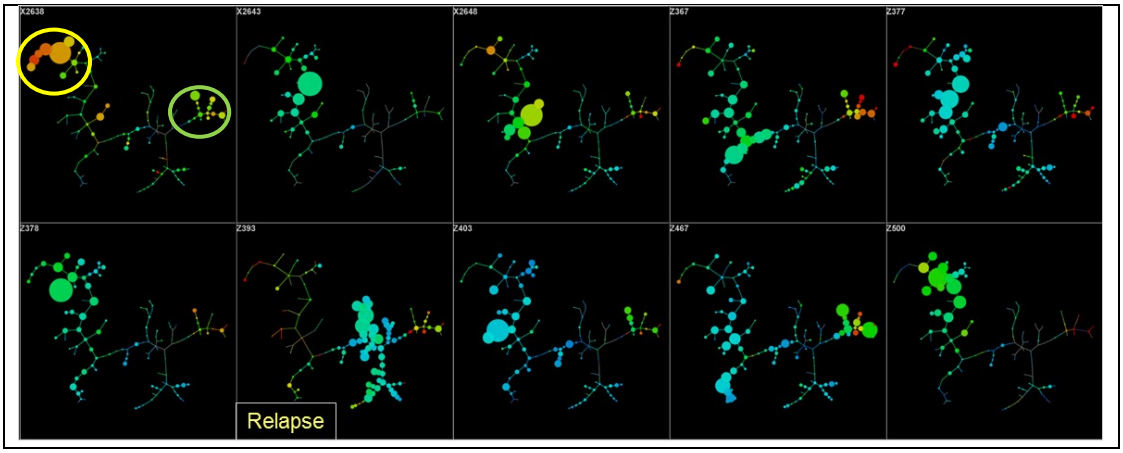

Figure 7: Minimum spanning tree shows **Sox2** expression. Scale is colored from 0 (blue) to 5 (red) and represents 0 to 95th percentile of the marker intensity distribution of individual cells. Sox 2 has consistent expression patterns within both the E-cadherin (yellow circle) and vimentin (green circle) compartments of the tumor

One of the main goals of this study is to delineate a cellular hierarchy for HG-SOC and relate the hierarchy to cellular functions such as tumorogenicity, metastasis and drug resistance. As mentioned above we have two large tumor samples with an excess of 50 million cells with which to do this. We will isolate cell subsets based on the information we gather from our tumor "landscaping study". Practical considerations will also be taken into account, especially the number of cells within a cluster. In some cases there may be too few. As part of our analysis in understanding biologically informative cluster, we performed hierarchical clustering based on the correlation between the expressions of each marker (Table 1) across all the tumors. The analysis yielded four "buckets of cell types" as shown in Figure 7. Interestingly, stem cell markers were distributed across all four "buckets". This is consistent with our data where stem cell markers such as CD133, CD61, CD49F etc, are distributed across many tumor cell subsets begging the hypothesis that "there are many ways to be a stem cell and that the ***combination,*** rather than any one stem cell marker alone, will be a critical determinant in regulating tumor function".

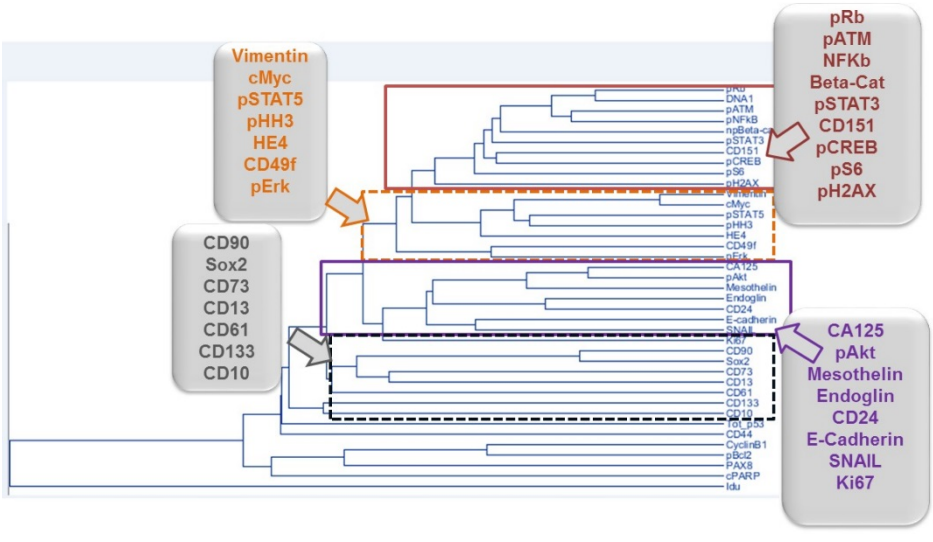

Figure 7: Hierarchical Clustering Based on Correlations of Expression Levels of Markers Across all Ten Tumors

C.2c Results from analyzing the immune compartment

The molecular diversity of HG-SOC presents a major challenge in designing effective targeted therapies and are more in line with per-patient designed strategies. Recent scientific evidence demonstrated that HG-SOC is an immunogenic tumor that can be recognized by the host

immune system [26]. However, in spite of this, immune evasion mechanisms persist [27]. Given the availability of agents that target such mechanisms (e.g anti-PD1, anti-PDL1 and anti-CTLA4 FDA-approved in several clinical setting), HG-SOC could be a prime candidate for targeted immune therapies. Thus, an understanding of the immune cell types as well as the interplay with the tumor cells could have a profound impact on the choice of immune-therapy.

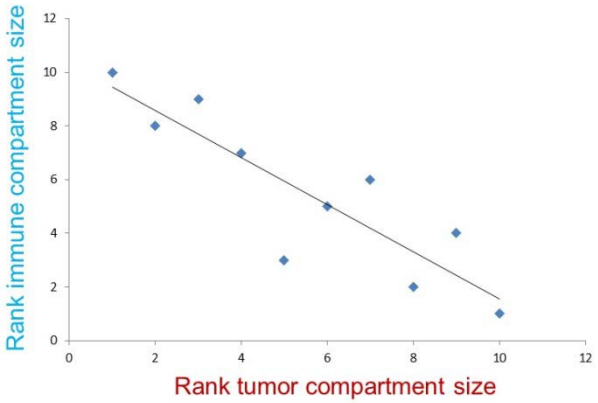

Figure 8: Tumor and immune compartment size are anti-correlated with a Spearman coefficient of -0.87

One question of interest in trying to understand the relationship between the tumor and immune compartments was how they influenced each other's size. Thus using, the tumor antibody panel in Table 1, we enumerated the cells in the CD45+ gate (immune compartment) and the CD45-/CD31-/FAP- gate and calculated their correlation. The plot in Figure 8 shows a strong anti-correlation between the immune and tumor compartments with a Spearman coefficient of -0.87.

At first glance these data suggest that a large immune compartment can keep the tumor at bay, whereas, a tumor thrives with a smaller immune compartment. Is this intuitive? The complex role of the immune system in tumor development, defined as "immuno-editing" can be divided into three sequential phases; *elimination, equilibration and escape [27]*. Thus from a functional standpoint the tight correlation we observed between the size of the two compartments might not have been anticipated. Perhaps size is independent of immune cell function because the cells adapt to the tumor and vice versa. Furthermore, using the antibody panel in Table 2, in the same experiment, we profiled the tumor immune system in the same ten tumors that we profiled with the tumor antibody panel (Table 1). We used peripheral blood mononuclear cells (PBMCs) from a healthy donor as a comparator. However, the ideal situation will be to compare the tumor immune system with matched patient PBMCs. We are in the process of acquiring those samples.

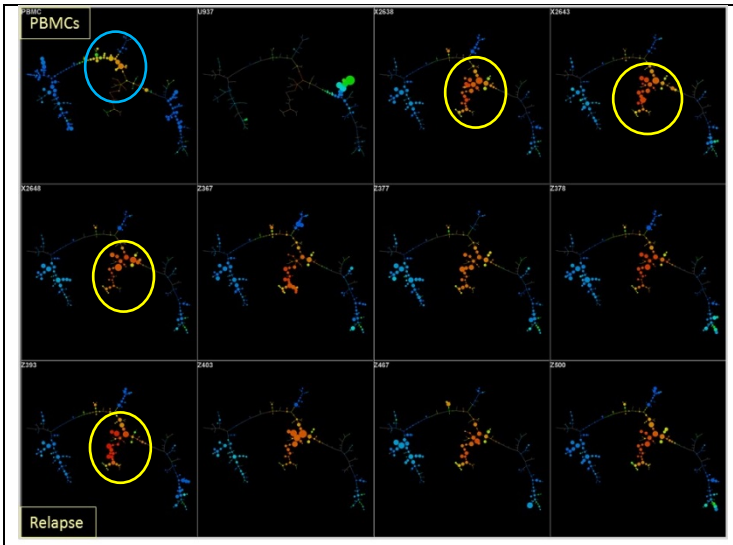

Figure 9: expression of CD68, a marker for macrophages. Top left panel PBMCs and adjacent panel U937 cells. Relapse sample shown bottom left. Yellow circle demarcates tumor macrophages and blue the comparable clusters in healthy PBMCs.

As with the tumor antibody panel, the data from the immune panel mass cytometry experiment was analyzed by X-shift k-nearest neighbor density-based clustering.

Immune cell types within the tumor whose abundance was greatly increased compared with healthy PBMCs were macrophages as shown by the levels of CD68 (Figure 8) and natural killer (NK) cells (data not shown). There were significant increases in expression patterns of various markers including ICOS, pSTAT1, pSTAT3, pCREB and pNFkB. A detailed analysis is ongoing.

With our mass cytometry profiling of the immune system in hand, we computed correlations between the sizes of the tumor compartments with specific immune cell subsets and found three NK cell subsets and one macrophage cell subset that correlated with the tumor compartment size (range of Spearman correlations 0.79 to 0.9). Remarkably, there was no correlation between the NK immune cells taken as an entity with the tumor compartment size. The identity of one NK cell cluster is shown in Figure 10 as an example. Of particular interest are the increases in pCREB, pSTAT1 and pNFKb (all targetable pathways) when compared to the comparable cell subsets within healthy PBMCs. When practically possible, we plan to cell-sort the immune cell subsets that correlate with size of the tumor compartment and develop in vitro co-culture assays to measure whether they are suppressive or permissive to tumor cell growth.

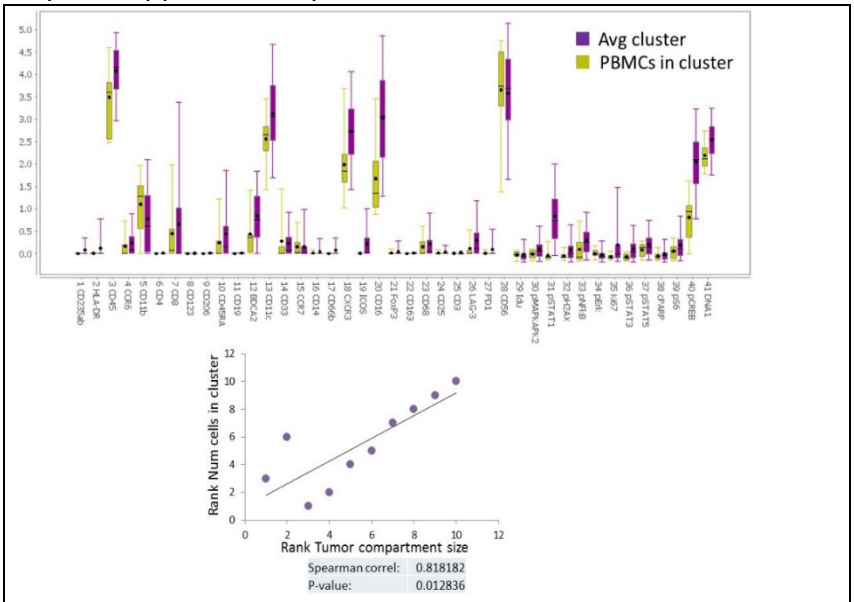

Figure 10: Example of Immune cell cluster in tumor that correlates with tumor cell size.

C.2d Functional assays

We have established the soft agar assay using the HG-SOC cell lines [11] as well as the MTT colorimetric proliferation assay. We have carried out the assays in the absence and presence of carboplatin, paclitaxel and JQ1 (data not shown). We are in a position to test our primary cells in these assays.

As mentioned above we are also establishing co-culture experiments to ascertain tumor-immune cell function in vitro

The Neel lab showed that from the initial rounds of CyTOF experiments, and by applying a novel algorithm developed by Dr. Pe'er, they identified several small populations of SOX2-containing cells in primary serous ovarian carcinoma (SOC) samples. Given the critical role of SOX2 in marking several different normal and cancer stem cell types, they hypothesized that SOX2+ populations might be enriched for ovarian tumor-initiating cells (TICs). These populations could be distinguished by surface markers, and most tumor samples had one or two different clusters; occasional cases had three. Interestingly, only some clusters were marked by CD133 expression, potentially consistent with the incomplete correlation between CD133 levels and ovarian TIC that we had reported earlier.

To be able to test the tumor-initiating capacity of SOX2+ cells, we developed a flow sorting strategy, using combinations of CD133, E-cadherin, CD90, and CD151, to enrich SOX2+ cells from different primary patient samples. Using this strategy, we screened eight different samples and sorted four of these into SOX2-enriched (up to 16-fold) vs SOX2-depleted subpopulations. We then performed LDAs to test whether SOX2 enrichment is correlated with higher TIC frequency. These experiments are now ongoing.

In parallel, we have attempted to develop *in vitro* surrogate assays for TICs, to shorten the enormous turnaround time imposed by conventional LDAs in mice. We adapted Clevers' organoid cultures and Schlegel's epithelial cell feeder method for primary serous ovarian cancer samples. In parallel to the LDA experiments described above, we placed sorted cells from each population into these *in vitro* culture systems. To assess whether organoid and colony formation *in vitro* correlates with TIC capacity. We also plan to inject (unsorted) organoids and

Schlegel colonies into NSG mice to assess further the relationship between *in vitro* growth and TIC capacity.

C2e Conditional density-based analysis of T cell signaling in single-cell data, a new computational approach developed collaboratively by the Pe'er and Nolan Labs

The premise of this study is that once we identify TILs and other drug resistant populations, we would characterize these cells and their potential vulnerabilities. We expect different subpopulations in the tumor to acquire different mechanisms to sustain growth and evade apoptosis, each such population uniquely altering signaling. Understanding precisely how signaling is altered can suggest treatment options. Therefore, we sought to develop a computational method that can characterize and compare signaling relations between subpopulations. Since the cancer signaling terrain not sufficiently characterized, we validated our methods on healthy immune data. The healthy immune system is especially well-suited for validation because it includes many rare subpopulations, that respond to signal differently, whose fraction in the population is similar to that of the tumor initiating cells that we wish to detect in ovarian cancer.

We developed methods for visualizing, identifying and scoring pairwise influences in single-cell data. We observed that classical statistical methods, such as mutual information, are unable to distinguish between spurious correlations and significant correlations because the majority of cells in a particular measurement may be inert or contain very similar levels of key molecules. However, in cancer it is often the minority of cells, or rare subpopulations that drive drug resistance or metastasis. Our methods are based on the analysis of the *conditional probability density* between a pair of molecules, an independent X molecule and a dependent Y molecule. Our method, known as DREVI (conditional-**D**ensity **R**escaled **V**isualization), enables the visual and mathematical characterization of signaling relations (Figure 1).

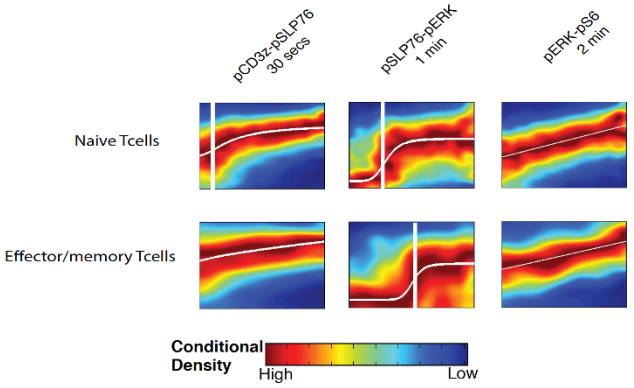

Fig 11. DREVI plots reveal differences in signaling interactions between naïve and effector/memory cells. Signaling response functions are altered between naïve and effector/ memory cells. Vertical lines show the threshold of inflection of the Y-molecule, which is altered between the two cell types. The white curves show the response function that cells follow.

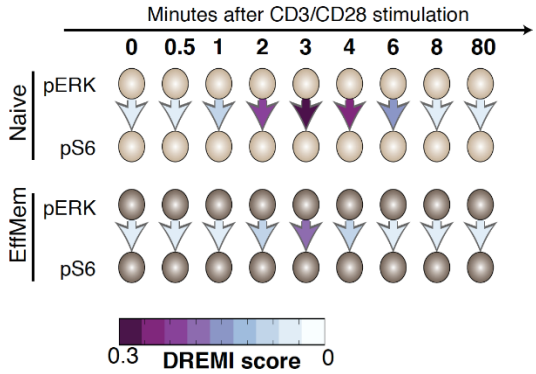

In addition, we develop a metric to quantify the strength of pairwise relationships known as DREMI (conditional-**D**ensity **R**esampled **E**stimate of **M**utual **I**nformation), so that one can robustly compare this metric between sub-polulations in the same tumor, between different conditions (drugged and undrugged), between tumors and between healthy and normal. Figure 2 shows the comparison of DREMI scores in a key-edge between two cell subtypes at various timepoints after T-cell receptor stimulation.

Fig 12. DREMI scores between 2-4 minutes show an increased dependence between pERK-pS6 in Naïve cells as compared to effector/memory cells.

We show that our methods are able to tease out subtle differences in signaling between related subtypes of peripheral T cells, naïve and effector/memory T cells, upon antigen engagement (See Fig 1.). Fig. 2 shows increased dependencies between pERK and pS6 in naïve cells. We successfully validated that this leads to a stronger impact upon knockout perturbation of ERK in naïve cells. This work was recently published in *Science [13]*. Our next step is to apply these methods to identify altered signaling subtypes in ovarian cancer cells.

D. KEY RESEARCH ACCOMLISHMENTS

- Established two validated antibody panels against the tumor and immune cell compartments.
- We conjugated 500ug of each antibody to ensure an adequate supply for analyzing future tumor specimens.
- Landscaped tumor and immune compartments of 10 primary HG-SOC tumors
- Landscaped ten HG-SOC cell lines selected from Domcke et al [11]
- All data highly reproducible
- Established MTT colorimetric proliferation assay
- Established growth in soft agar assay
- Developed new computational tools: X-shift (unpublished) CITRUS [12]DREMI [13], allof which will be used to analyze the mass cytometry data sets of HG-SOC

E. CONCLUSIONS

- See tumor diversity between samples, but within *a limited phenotypic hierarchy*
  - For both surface markers and signaling molecules
- See mutually exclusive expression of E-cadherin and vimentin in “epithelial” and “mesenchymal” compartments
- Stem cell markers scattered throughout compartments: are there many ways to be a stem cell? Functional analysis can help answer this
- Great diversity in size of immune compartment across samples
- Even with ten samples, we see a correlation between a tumor cell type with immune compartment size and immune cell type with tumor compartment size.
- Size of tumor and immune compartments anti-correlated
- Three NK cell subsets and one macrophage cell subset are positively correlated with tumor compartment size
- No correlation exists between NK cells and size of tumor compartment
- Highly regulated communication between immune and tumor compartments
- New level of detail revealed by multi-parametric single cell mass cytometry.

F. PUBLICATIONS AND TALKS

1. Bjornson ZB, **Nolan GP**, Fantl WJ. Single-cell mass cytometry for analysis of immune system functional states. Curr Opin Immunol. 2013 Aug;25(4):484-94. doi: 10.1016/j.coi.2013.07.004. Epub 2013 Aug 31. Review. PubMed PMID: 23999316; PubMed Central PMCID: PMC3835664.

2. Kinoshita SM, Kogure A, Taguchi S, **Nolan GP**. Snapin, positive regulator of stimulation- induced Ca^{2+} release through RyR, is necessary for HIV-1 replication

in T cells. PLoS One. 2013 Oct 10;8(10):e75297. doi: 10.1371/journal.pone.0075297. eCollection 2013. PubMed PMID: 24130701; PubMed Central PMCID: PMC3794929.

3. Wolchinsky R, Hod-Marco M, Oved K, Shen-Orr SS, Bendall SC, **Nolan GP**, Reiter Y. Antigen-dependent integration of opposing proximal TCR-signaling cascades determines the functional fate of T lymphocytes. J Immunol. 2014 Mar 1;192(5):2109-19. doi: 10.4049/jimmunol.1301142. Epub 2014 Jan 31. PubMed PMID: 24489091.

4. Sachs K, Itani S, Fitzgerald J, Schoeberl B, **Nolan GP**, Tomlin CJ. Single timepoint models of dynamic systems. Interface Focus. 2013 Aug 6;3(4):20130019. doi: 10.1098/rsfs.2013.0019. PubMed PMID: 24511382; PubMed Central PMCID: PMC3915837.

5. Fienberg HG, **Nolan GP**. Mass cytometry to decipher the mechanism of nongenetic drug resistance in cancer. Curr Top Microbiol Immunol. 2014;377:85-94. doi: 10.1007/82_2014_365. Review. PubMed PMID: 24578267.

6. Angelo M, Bendall SC, Finck R, Hale MB, Hitzman C, Borowsky AD, Levenson RM, Lowe JB, Liu SD, Zhao S, Natkunam Y, **Nolan GP**. Multiplexed ion beam imaging of human breast tumors. Nat Med. 2014 Apr;20(4):436-42. doi: 10.1038/nm.3488. Epub 2014 Mar 2. PubMed PMID: 24584119; PubMed Central PMCID: PMC4110905.

7. Bendall SC, Davis KL, Amir el-AD, Tadmor MD, Simonds EF, Chen TJ, Shenfeld DK, **Nolan GP**, Pe'er D. Single-cell trajectory detection uncovers progression and regulatory coordination in human B cell development. Cell. 2014 Apr 24;157(3):714-25. doi: 10.1016/j.cell.2014.04.005. PubMed PMID: 24766814; PubMed Central PMCID: PMC4045247.

8. Bruggner RV, Bodenmiller B, Dill DL, Tibshirani RJ, **Nolan GP**. Automated identification of stratifying signatures in cellular subpopulations. Proc Natl Acad Sci U S A. 2014 Jul 1;111(26):E2770-7. doi: 10.1073/pnas.1408792111. Epub 2014 Jun 16. PubMed PMID: 24979804; PubMed Central PMCID: PMC4084463.

9. Pyne S, Lee SX, Wang K, Irish J, Tamayo P, Nazaire MD, Duong T, Ng SK, Hafler D, Levy R, **Nolan GP**, Mesirov J, McLachlan GJ. Joint modeling and registration of cell populations in cohorts of high-dimensional flow cytometric data. PLoS One. 2014 Jul 1;9(7):e100334. doi: 10.1371/journal.pone.0100334. eCollection 2014. PubMed PMID: 24983991; PubMed Central PMCID: PMC4077578.

10: Sen N, Mukherjee G, Sen A, Bendall SC, Sung P, **Nolan GP**, Arvin AM. Single-cell mass cytometry analysis of human tonsil T cell remodeling by varicella zoster virus. Cell Rep. 2014 Jul 24;8(2):633-45. doi: 10.1016/j.celrep.2014.06.024. Epub 2014 Jul 17. PubMed PMID: 25043183; PubMed Central PMCID: PMC4127309.

11. Fienberg HG, **Nolan GP**. High-dimensional cytometry. Preface. Curr Top Microbiol Immunol. 2014;377:vii-viii. PubMed PMID: 25118348.

12. Gaudillière B, Fragiadakis GK, Bruggner RV, Nicolau M, Finck R, Tingle M, Silva J, Ganio EA, Yeh CG, Maloney WJ, Huddleston JI, Goodman SB, Davis MM, Bendall SC, Fantl WJ, Angst MS**, Nolan GP**. Clinical recovery from surgery correlates with single-cell immune signatures. Sci Transl Med. 2014 Sep 24;6(255):255ra131. doi: 10.1126/scitranslmed.3009701. PubMed PMID: 25253674.

13. Behbehani GK, Thom C, Zunder ER, Finck R, Gaudilliere B, Fragiadakis GK, Fantl WJ, **Nolan GP**. Transient partial permeabilization with saponin enables cellular barcoding prior to surface marker staining. Cytometry A. 2014 Oct 1. doi: 10.1002/cyto.a.22573. [Epub ahead of print] PubMed PMID: 25274027.

14. Sachs Z, LaRue RS, Nguyen HT, Sachs K, Noble KE, Mohd Hassan NA, Diaz-Flores E, Rathe SK, Sarver AL, Bendall SC, Ha NA, Diers MD, **Nolan GP**, Shannon KM, Largaespada DA. NRASG12V oncogene facilitates self-renewal in a murine model of acute myelogenous leukemia. Blood. 2014 Oct 14. pii: blood-2013-08-521708. [Epub ahead of print] PubMed PMID: 25316678.

15. Krishnaswamy S, Spitzer MH, Mingueneau M, Bendall SC, Litvin O, Stone E, Pe'er D, **Nolan GP**. Conditional density-based analysis of T cell signaling in single-cell data. Science. 2014 Oct 23. pii: 1250689. [Epub ahead of print] PubMed PMID: 25342659.

16. Zunder E, Finck R, Behbehani GK, Amir ED, Krishnaswamy S, Gonzalez VD, Lorang CG, Bjornson Z, Spitzer MH, Bodenmiller B, Fantl WJ, Pe'er D, **Nolan GP**. Palladium-based Mass-Tag Cell Barcoding with a Doublet-Filtering Scheme and Single Cell Deconvolution Algorithm. Nature methods. **In press.**

TALKS

Nolan

Nolan: Washington University Department of Medicine Seminar, September 10, 2013, **The Structure of Immunity and Cancer at the Single Cell level**, St. Louis, MO

Nolan: Advances and Perspectives on Flow Cytometry 2013, September 20, 2013, **Mass Cytometry and Cell Cycle**, Mexico City, Mexico (by Web Conference)

Nolan: Nuclear Reprogramming and the Cancer Genome, **Reprogramming: Induced Pluripotent Stem Cells**, St. Catherine's College, Oxford, England

Nolan: Inserm Workshop 225, October 2, 2013, **A Definable "Structure" for the Immune System and Cancers at the Single Cell Level**, Bordeaux, France

Nolan: American Society for Human Genetics – Medical Systems Genomics, October 26, 2013, **Single Cell Systems-Structured View of Immunity & Cancer,** Boston, MA

Nolan: 2013 ACR/ARHP Annual Meeting, October 25-30, 2013, **Emerging Technologies for Defining Immune Signatures**, San Diego, CA

Nolan: 8th Cell Based Assay & Screening Technologies Conference, Nov. 6-8, 2013, **A Definable "Structure" for the Immune System and Cancers at the Single Cell Level**, San Francisco, CA

Nolan: Columbia University Microbiology & Immunology, November 20, 2013, **A Definable "Structure" for the Immune System and Cancers at the Single Cell Level**, New York, NY
Nolan: NCI ICBP Current Topics in Cancer Systems Biology: Tumor Cell Heterogeneity Workshop, December 2, 2013, **A systems structured view of immunity and cancer**, Vanderbilt University, Nashville, TN

Nolan: American Society for Cell Biology (ASCB) Annual Meeting, December 14, 2013, **Deconvoluting the complexities of cancer through physical sciences based single-cell approaches**, New Orleans, LA

Nolan: NCI Workshop on RAS: Synthetic Lethality Screens for Finding KRAS Vulnerabilities, January 9, 2014, **Modern approaches to single cell analysis**, Frederick, MD

Nolan: Harvard Medical School – Program in Immunology Seminars, February 5, 2014, **Mass Cytometry: Next generation flow cytometry**, Cambridge, MA

Nolan: Massachusetts General Hospital – Immunology Seminar Series, February 6, 2014, **Mass Cytometry: Next generation flow cytometry**, Charlestown, MA

Nolan: Society for Hematopathology, March 2, 2014, **New Technologies Applicable to Study of T-cell lymphomas: Taking Flow Cytometry to the next level – deciphering T-cell function**, San Diego, CA

Nolan: Penn Genome Frontiers Institute – Single Cell Symposium, March 11, 2014, **A single cell systems view of immunity and cancer**, Philadelphia, PA

Nolan: AACR Annual Meeting, April 7, 2014, **A single cell systems-structured for cancer and immunity**, San Diego, CA

Nolan: Stanford Translational Research and Applied Medicine Program (TRAM), May 16, 2014, **A Systems-Structured View of Immunity & Cancer,** Stanford University, CA

Nolan: U. Minnesota – Department of Biochemistry, Molecular Biology and Biophysics (BMBB), May 20, 2014, **Mass Cytometry: Next generation flow cytometry**, Minneapolis, MN

Nolan: Academy of Clinical Laboratory Physicians & Scientists – Cotlove Award Lecture, May 30, 2014, **A structure for immunity and cancer at the single level**, San Francisco, CA

Nolan: 2014 MCMi Regulatory Science Symposium Keynote, June 2, 2014, **A structure for immunity and cancer at the single level**, FDA Headquarters, Silver Springs, MD

Nolan: NCI Workshop on RAS Pathway Modeling and Quantitative Measurements, June 11, 2014, **Analysis of Signaling Networks at the Single Cell Level**, NIH Campus, Bethesda, MD

Nolan: Harvard Medical School – Center for Cancer Systems Biology, June 12, 2014, **Single-cell, tissue-organized, systems-structured views of immunity and cancer**, Boston, MA

Nolan: Fluidigm Symposium – To revolutionize Regenerative Medicine and Oncology by single cell analysis, June 17, 2014, **Mass Cytometry: Next generation flow cytometry**, Tokyo, Japan
Nolan: Nature – Genomic Technologies and Biomaterials for Understanding Disease, June 23, 2014. **A definable "structure" for the immune system and cancers at the single cell level**, San Diego, CA

Nolan: Banbury Center – The Immune System and Cancer, September 9, 2014, **Single Cell proteomics and genomics at high scale**, Cold Spring Harbor Laboratory, NY

Nolan: Trinity College Symposium – Translating Imaging and other Novel Approaches, September 17, 2014, **A structure for immunity and cancer at the single level**, Oxford, England

Fantl

1. **Fantl WJ.** Invited speaker, ASH, New Orleans December 7th 2013. **All Roads Lead to Rome: Phenotypic Channeling to Uniform Differentiation Structures from Diverse Leukemia Genotypes by Mass Cytometry.**

2. **Fantl WJ.** Invited speaker, 2014 Frontiers in Biomedical Research Symposium, Scripps Research Retreat, Palm Desert, CA, February 17th 2014. **Single Cell Systems-Structured View of Immunity and Cancer.**

3. **Fantl WJ.** Invited speaker, Stratified Medicine Symposium, London, UK July 10th 2014. **Single Cell Structured View of Immunity and Cancer.**

4. **Fantl WJ.** Invited *keynote* speaker, Novel Technologies for in vitro Diagnostics, Leuven Belgium October 2014. **Single Cell Structured View of Immunity and Cancer.**

Neel

Neel B AACR Advances in Ovarian Cancer Conference, Sept 20, 2013: **Cellular Heterogeneity in High-Grade Serous Ovarian Cancer.**

Neel B Banbury conference: April 21-23 2014. **Patient-derived xenografts for analyzing tumor-initiating cells and drug response in high grade serous ovarian cancer.**

Neel B AACR Annual Meeting: Current Concepts in Organ Site Research Section. April 2014
A Systems approach to Serous Ovarian Cancer.

G. INVENTIONS PATENTS AND LICENSES
N/A

H. REPORTABLE OUTCOMES
N/A

I. OTHER ACHIEVEMENTS
N/A

REFERENCES

1. Bowtell, D.D., *The genesis and evolution of high-grade serous ovarian cancer.* Nat Rev Cancer, 2010. **10**(11): p. 803-8.
2. Berns, E.M. and D.D. Bowtell, *The changing view of high-grade serous ovarian cancer.* Cancer Res, 2012. **72**(11): p. 2701-4.
3. *Integrated genomic analyses of ovarian carcinoma.* Nature, 2011. **474**(7353): p. 609-15.
4. Tothill, R.W., et al., *Novel molecular subtypes of serous and endometrioid ovarian cancer linked to clinical outcome.* Clin Cancer Res, 2008. **14**(16): p. 5198-208.
5. Vogelstein, B., et al., *Cancer genome landscapes.* Science, 2013. **339**(6127): p. 1546-58.
6. Bendall, S.C., et al., *A deep profiler's guide to cytometry.* Trends Immunol, 2012. **33**(7): p. 323-32.
7. Bendall, S.C., et al., *Single-cell mass cytometry of differential immune and drug responses across a human hematopoietic continuum.* Science, 2011. **332**(6030): p. 687-96.
8. Bjornson, Z.B., G.P. Nolan, and W.J. Fantl, *Single-cell mass cytometry for analysis of immune system functional states.* Curr Opin Immunol, 2013. **25**(4): p. 484-94.
9. Tanner, S.D., et al., *An introduction to mass cytometry: fundamentals and applications.* Cancer Immunol Immunother, 2013. **62**(5): p. 955-65.
10. Ornatsky, O., et al., *Highly multiparametric analysis by mass cytometry.* J Immunol Methods, 2010. **361**(1-2): p. 1-20.
11. Domcke, S., et al., *Evaluating cell lines as tumour models by comparison of genomic profiles.* Nat Commun, 2013. **4**: p. 2126.
12. Bruggner, R.V., et al., *Automated identification of stratifying signatures in cellular subpopulations.* Proc Natl Acad Sci U S A, 2014. **111**(26): p. E2770-7.
13. Krishnaswamy, S., et al., *Conditional density-based analysis of T cell signaling in single-cell data.* Science, 2014.
14. Bodenmiller, B., et al., *Multiplexed mass cytometry profiling of cellular states perturbed by small-molecule regulators.* Nat Biotechnol, 2012.
15. Fienberg, H.G., et al., *A platinum-based covalent viability reagent for single-cell mass cytometry.* Cytometry A, 2012. **81**(6): p. 467-75.
16. Finck, R., et al., *Normalization of mass cytometry data with bead standards.* Cytometry A, 2013. **83**(5): p. 483-94.
17. Davidson, B., C.G. Trope, and R. Reich, *Epithelial-mesenchymal transition in ovarian carcinoma.* Front Oncol, 2012. **2**: p. 33.
18. Kalluri, R. and R.A. Weinberg, *The basics of epithelial-mesenchymal transition.* J Clin Invest, 2009. **119**(6): p. 1420-8.
19. Tam, W.L. and R.A. Weinberg, *The epigenetics of epithelial-mesenchymal plasticity in cancer.* Nat Med, 2013. **19**(11): p. 1438-49.
20. Tan, T.Z., et al., *Epithelial-mesenchymal transition spectrum quantification and its efficacy in deciphering survival and drug responses of cancer patients.* EMBO Mol Med, 2014. **6**(10): p. 1279-93.
21. Simmons, A.R., K. Baggerly, and R.C. Bast, Jr., *The emerging role of HE4 in the evaluation of epithelial ovarian and endometrial carcinomas.* Oncology (Williston Park), 2013. **27**(6): p. 548-56.
22. Schummer, M., et al., *Evaluation of ovarian cancer remission markers HE4, MMP7 and Mesothelin by comparison to the established marker CA125.* Gynecologic oncology, 2012. **125**(1): p. 65-9.

23. Hassan, R., et al., *Phase 1 study of the antimesothelin immunotoxin SS1P in combination with pemetrexed and cisplatin for front-line therapy of pleural mesothelioma and correlation of tumor response with serum mesothelin, megakaryocyte potentiating factor, and cancer antigen 125.* Cancer, 2014. **120**(21): p. 3311-9.
24. Pastan, I. and R. Hassan, *Discovery of mesothelin and exploiting it as a target for immunotherapy.* Cancer Res, 2014. **74**(11): p. 2907-12.
25. Chekmasova, A.A., et al., *Successful eradication of established peritoneal ovarian tumors in SCID-Beige mice following adoptive transfer of T cells genetically targeted to the MUC16 antigen.* Clin Cancer Res, 2010. **16**(14): p. 3594-606.
26. Zsiros, E., et al., *Immunotherapy for ovarian cancer: recent advances and perspectives.* Curr Opin Oncol, 2014. **26**(5): p. 492-500.
27. Mittal, D., et al., *New insights into cancer immunoediting and its three component phases--elimination, equilibrium and escape.* Curr Opin Immunol, 2014. **27**: p. 16-25.